The rapid response of 2/1 tearing mode to electrode biasing in J-TEXT experiments

Tong Wang[1], Zhipeng Chen[1,*], Qiming Hu[2], Hai Liu[3], Q. Yu[4], Jie Yang[1], Mingxiang Huang[1], Da Li[1], Chengshuo Shen[1], Yuan Huang[1], Minghui Xia[1], Zhifeng Cheng[1], Li Gao[1], Zhoujun Yang[1], Lizhi Zhu[1], Yonghua Ding[1], Nengchao Wang[1], Peng Shi[1], Zhongyong Chen[1], G. Zhuang[5], Yunfeng Liang[1] and the J-TEXT Team

[1]International Joint Research Laboratory of Magnetic Confinement Fusion and Plasma Physics, State Key Laboratory of Advanced Electromagnetic Engineering and Technology, School of Electrical and Electronic Engineering, Huazhong University of Science and Technology, Wuhan, 430074, China

[2] Princeton Plasma Physics Laboratory, Princeton NJ 08543-0451, USA

[3] Institute of Fusion Science, Southwest Jiaotong University, Chengdu, 610031, China

[4] Max-Planck-Institut für Plasmaphysik, 85748, Garching, Germany

[5] Department of Engineering and Applied Physics School of Physical Sciences, University of Science and Technology of China, Hefei Anhui, 230026, China.

*Corresponding author E-mail: zpchen@hust.edu.cn

Abstract

The electrode biasing (EB) has been applied to modulate the m/n = 2/1 tearing modes (TM) in J-TEXT tokamak, where m and n are the poloidal and toroidal mode numbers. According to the response time, the response of 2/1 tearing mode frequency to EB can be divided into two processes, the rapid response and the slow response. In the rapid response, experimental results show that the variation of mode frequency is ahead of the variation of plasma rotation, which is analogous to the result mentioned in paper [1]. Statistic results indicate that the rapid response coefficient of TM frequency to EB current is a constant. The detailed analysis of rapid response obtained by auto-conditional average shows that the mode frequency varying lags about 13 μs behind of the variation of current. What's more is that the mode frequency derivative increases in proportion with the increase of the EB current value. A heuristic mechanism of the rapid response of 2/1 tearing mode to electrode biasing is presented, which is relevant to the rotation difference between magnetic island and edge plasma layer rather than the flow shear around the magnetic island. The experimental results suggest that the application of electrode biasing can modulate the TM frequency in a small amount of time, which is a possible method for the avoidance of mode locking and disruption.

Keywords: tearing mode, electrode biasing, plasma rotation, MHD instability, disruption avoidance

(Some figures may appear in color only in the electronic version)

1. Introduction

The onset of the tearing mode (TM) or neoclassic tearing mode (NTM) can degrade the tokamak confinement. Mode locking and major disruption will happen if the mode amplitude is sufficiently large, which will be an important issue to be solved for a fusion reactor. Experimental and numerical results show that the localized drive or heating can stabilize the mode. In addition, disruption avoidance by stabilizing the TM has also attracted many researchers.

Among theoretical analysis, many researches are concentrated on the effect of plasma flow (or flow shear) on the TM. Some studies show that the flow shear affects MHD modes and the shape of the magnetic island by the viscous drag[2-8]. An interesting thing is that the flow shear can either increase or decrease the TM growth rate, which depends on the plasma viscosity, the magnetic shear, and the strength of flow shear[2-11]. However, It is also found that the plasma performance and MHD instability depended more on the plasma rotation at the resonant surface rather than on the flow shear[12]. A recent numerical simulation indicates that weak or moderate flow shear can decrease the TM growth rate in the linear phase and lead to a smaller saturated island width in the nonlinear phase[10].

A number of experimental studies have examined the effect of shear plasma flow on tearing mode. Many results show that the existence of flow shear will increase the stability of TM and make pre-exist saturated island smaller[13-15]. The varying mix of co- and counter-neutral beams injection (NBI) is applied to change the rotation on DIII-D, showing that flow shear would make the effective tearing stability index △' more negative and then stabilize the m/n = 3/2 neoclassical tearing mode[16-18]. On JET, it is found that the higher rotation can increase the beta for NTM onset and make the tearing mode more stabilizing[19]. On NSTX, the plasma rotation is also found to stabilize the m/n = 3/2 mode [20]. In some medium or small size tokamaks, the plasma parameters and flows are changed by the biased electrode[21-28]. Suppression of MHD activity with electrode[26] or limiter biasing[27, 28] has been observed in experiments. There is clear yet again an advantage for improved tearing stability by having strong applied torque and driving large rotation.

On J-TEXT tokamak, an electrode biasing (EB) system for driving plasma rotation has been designed and installed, being able to insert into the plasma by a reciprocating drive during the discharge[1, 29-31]. It is found that the 2/1 TM is stabilized with the increased toroidal plasma rotation speed in the counter-Ip direction for a negative bias voltage[1]. In this paper, the previous work is extended to settle the question mentioned in paper [1], which is that the TM frequency decouples from V_Φ. According to the response time, the response of 2/1 tearing mode to EB can be divided into two processes, the rapid response and the slow response. The experimental results show that the effect of EB on mode frequency isn't caused by flow shear or flow in the rapid phase, because the rapid response time doesn't conform to the time of momentum transport process.

This paper is organized as follows: the experimental setup is given in section 2.1. The effect of EB parameters on TM frequency is presented in section 2.2. The section 2.3 is mainly devoted to the dynamics of rapid response of TM frequency to EB current. A brief discussion is given in section 3 and the summary is presented in section 4.

2. Experimental results

2.1. Experimental setup

The experiments are carried out in Ohmic hydrogen discharges on J-TEXT tokamak with a limiter configuration (major radius R_0 = 105cm and minor radius a = 25.5cm)[32]. Unless otherwise stated, the plasma parameters are as followed: plasma current Ip = 175 kA, toroidal magnetic field B_t = 1.6 T, the safety factor q_a = 2.83 at the plasma edge, and the central line-averaged electron density n_e~1-2×10^{19} m^{-3}. In these discharges an m/n = 2/1 TM grows and saturates before the application of EB. This mode rotates in the electron diamagnetic drift direction with a frequency of 4 kHz.

The electrode biasing system is installed at a midplane port on the low field side (LFS), as shown in paper [1, 29-31]. A graphite electrode is mounted on the head of the EB and inserted into the plasma by a reciprocating drive during the discharge at the location of r = 23.5~25.5 cm, that is 0~2 cm inside the last closed flux surface (LCFS). The bias voltage (U_{EB}) applied on the electrode with respect to the vacuum vessel wall is in the range of −500 to +150 V.

The edge toroidal rotation of Carbon V (i.e. C^{+4}) impurity is measured by the multi-channel spectrometer[33] in the range of r/a = 0.65~1. The m/n = 2/1 TM is measured by poloidal and toroidal

Mirnov arrays and identified from the temporal evolution of the Mirnov signals using singular value decomposition (SVD) technique[34]. The q = 2 rational surface is at approximate $r \sim 19$ cm (i.e. r/a = 0.74), which is estimated by the reverse radius of electron temperature perturbation measured by electron cyclotron emission (ECE)[35] .

2.2. Effect of EB parameters on TM frequency

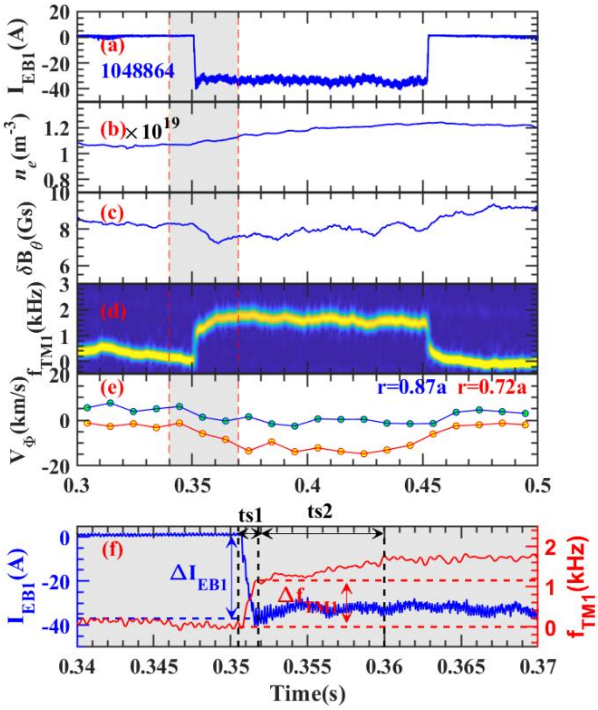

Figure 1. Time evolutions of (a) current of electrode biasing (I_{EB1}); $I_{EB1}=I_{EB}-I_{EB0}$, I_{EB0} is the EB current before the application of bias voltage at about 0.35s; (b) central line-averaged electron density (n_e); (c) poloidal magnetic perturbation(δB_θ); (d) m/n=2/1 Mirnov toroidal rotation frequency (f_{TM1}); $f_{TM1}=f_{TM}-f_{TM0}$, f_{TM0} is the TM frequency before the application of bias voltage at about 0.35; (e) carbon V toroidal velocities V_Φ at r=0.72a and 0.87a, while the island is located at about 0.74a for shot 1048864. (f) The detailed analyses of EB current (by blue curve) and tearing mode frequency (by red curve), $\triangle f_{TM1}$ and $\triangle I_{EB1}$ defined in figure 1(f), are variations before and after the application of EB.

A typical phenomenon of the effect of electrode biasing on the 2/1 TM is shown in figure 1. The EB has been inserted into plasma and stayed at 245mm before applying bias voltage (U_{EB}=-200V) for 1048864. Figure 1(a) shows the EB current of the shot 1048864, the bias current is turned on at about t = 0.35s, ramped up to the flattop at t=0.351s and turned off at t = 0.45s. Figure 1(b) displays the central line-averaged electron density from 0.3s to 0.5s with slight change. The time evolutions of the poloidal magnetic field perturbation and TM toroidal frequency are shown in figures 1(c)-(d). $f_{TM1}>0$ means that the TM frequency and stabilization increase with the application of EB. When the bias current exists, the f_{TM1} increases from about 0 kHz to about 2 kHz with the magnetic perturbation amplitude of the 2/1 TM suppressed firstly and then increased slowly. However, the mode frequency changes much faster than the mode amplitude varying when turning on/off the EB current. The toroidal plasma rotation velocities V_Φ measured by multi-channel spectrometer at two different radial positions (r/a = 0.72, 0.87, while the island is located at about 0.74a.) are displayed in figure 1(e). The toroidal rotation speed increases in the counter-I_p direction with negative variation of EB current, where the positive value corresponds to the co-I_p direction. It's clear that the variation of mode frequency is asynchronous with the variation of plasma rotation, which is similar to the results mentioned in [1]. The shaded part shows the rapid response of 2/1 TM to EB from 0.34s to 0.37s, which is displayed in figure 1(f) in detail.

As shown in figure 1(f), the f_{TM1}, which is shown by the red line, increases rapidly from 0 kHz to

1.2 kHz as the EB current (shown by blue curve) increasing. When the EB current is on the flattop and keeps stable, the f_{TM1} increases slowly from 1.2 kHz to about 1.9 kHz and then maintains at the same level. According to the response time, the reaction of the mode frequency to EB current can be divided into two processes. First, the TM frequency is affected by the increase of EB current within milliseconds (ts1), which changes fast, and is called the rapid response. Then, the TM frequency increases slowly while EB current almost keeps steady during about tens of milliseconds (ts2), and we call it slow response. For the slow response, the mode frequency and amplitude vary synchronously with the plasma rotation. The possible explanation is that the slow response is caused by flow or flow shear around the magnetic island. For the rapid response, the mode frequency is asynchronous with the variation of plasma rotation and mode amplitude, which shows that the mechanism of the rapid response isn't similar to that of the slow one.

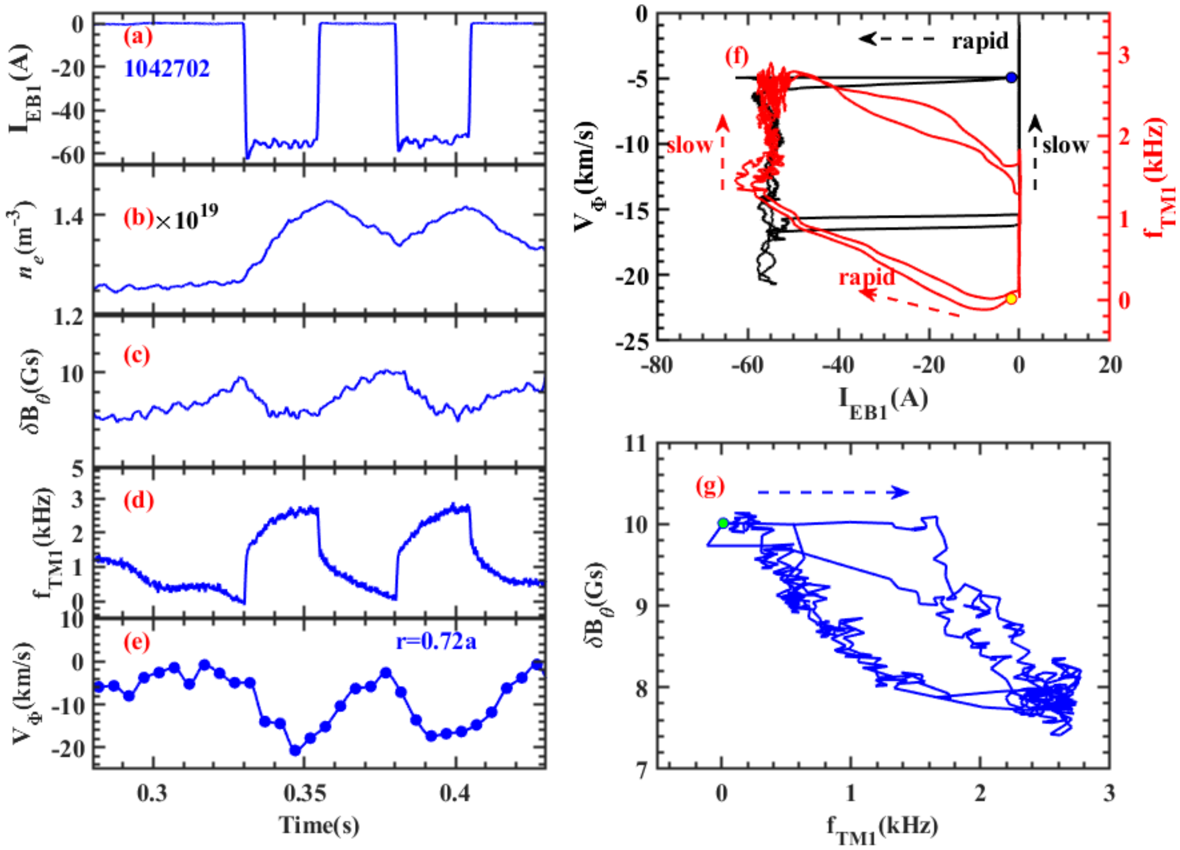

Figure 2. Time evolutions of (a) current of electrode biasing (I_{EB1}), (b) central line-averaged electron density (n_e), (c) poloidal magnetic perturbation (δB_θ), (d) TM frequency (f_{TM1}), (e) carbon V toroidal velocity V_Φ at r=0.72a for shot 1042702. (f) Tearing mode frequency (by red curve) and toroidal velocity (by black curve) versus EB current. (g) Poloidal magnetic perturbation versus tearing mode frequency.

As mentioned in paper [1], the modulated current is applied to study the repeatability of the response with Ip = 165 kA and B_t = 1.6 T, as shown in figure 2. The plasma parameters (n_e, V_Φ) and TM parameters (f_{TM1}, δB_θ) vary periodically with the modulated EB current. Periodic stabilization of TM (figure 2(c)) is seen together with the increase of the TM frequency (figure 2 (d)) for negative EB current. There are periodic rapid and slow responses of mode frequency to current as periodically turning on/off the bias. However, the TM frequency increases in about 1ms at the rapid response, which is much faster than the variations of other plasma parameters. The hysteresis loops of the plasma rotation (black curve) and tearing mode frequency (red curve) versus EB current from 0.33s to 0.43s are shown in figure 2(f). The arrows mean the directions of the loops with the initial points shown by circles. In the rapid response, the mode frequency varies much faster than plasma rotation, which means that the rapid mode frequency changing is independent of the plasma rotation. In figure 2(g), the mode amplitude decreasing/increasing lags behind the mode frequency increasing/decreasing, which reveals that as the mode frequency increasing/decreasing, the flow or flow shear around the island increases/decreases to decrease/increase the amplitude of the island.

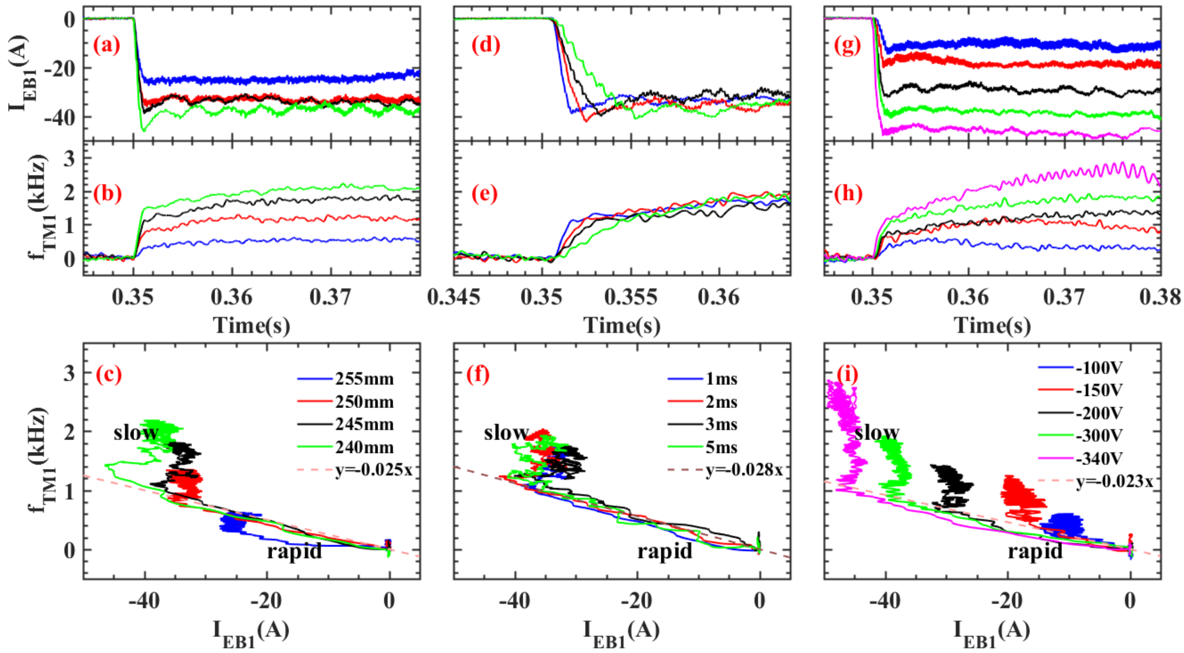

Figure 3. The effect of EB current (I_{EB1}) on TM frequency (f_{TM1}) for different EB positions (P_{EB}), EB current rise time (t_{EB}) and bias voltages (U_{EB}). For every situation, the only variable EB parameter is shown by different colors while the others keeping the same. (a), (d), (g) Time evolutions of EB current (I_{EB1}); (b), (e), (h) time evolutions of TM frequency (f_{TM1}); (c), (f), (i) tearing mode frequency versus EB current.

A set of experiments have been carried out to explore the effect of EB parameters on mode frequency. The effects of different EB position, EB current rise time and bias voltage on TM frequency are shown in figures 3(a)-(c), figures 3(d)-(f) and figures 3(g)-(f), respectively.

The figures 3(b)-(c) show the effect of different electrode locations on TM frequency with negative bias voltage (-200V) while the EB current rise time is 1ms to make the rapid response and the slow response more discernible. It's found that as the positions of electrode going deeper, the plasma density increases to make the EB current raising figure 3(a). While the bias voltages keep constant, TM frequency rises with EB current increasing, which reveals that the mode frequency is related to the EB current. As shown in figure 3(c), the dashed line means the fitting curve for the relation between f_{TM1} and I_{EB1}, which is $f_{TM1} = -0.025 \times I_{EB1}$. The rapid response coefficients of f_{TM1} to I_{EB1} are similar when the electrode enters into the plasma (while the positions=240mm, 245mm, 250mm). However, the response represented is much weaker when the electrode is at the last closed flux surface (position=255mm).

The figures 3(e)-(f) show the response of mode frequency to EB current for different EB current rise time with negative bias voltage (-200V) while the position is 245mm. The more EB current rise time is, the more variation time of mode frequency is. On account of the similar values of four shots' EB current (figure 3(d)) after rapid and slow response, the values of TM frequency (figure 3(e)) are all about 1.2 kHz and 1.9 kHz, respectively. It's found that TM frequency have a linear relation with EB current for different EB current rise time in the 'rapid' process, $f_{TM1} = -0.028 \times I_{EB1}$, which is similar to that presented in the figure 3(c).

Another experiment has been carried out by keeping position of electrode biasing at 245mm and the EB current rise time 1ms, while only the bias voltage scans from -340 to -100V. In figures 3(g)-(h), it's found that values of EB current and TM frequency raise as the bias voltages increasing. The fitting curve of f_{TM1} versus I_{EB1}, $f_{TM1} = -0.023 \times I_{EB1}$, is shown by dashed line in figure 3(i). The rapid response of TM frequency to EB current is a linear dependence, which is similar to the results mentioned in figures 3(c) and (f).

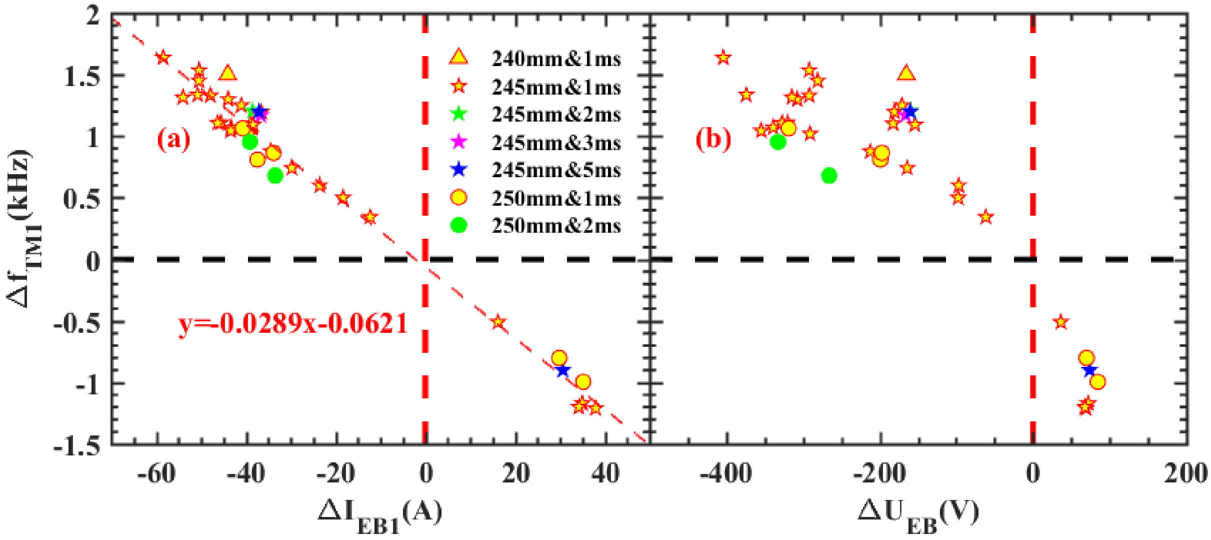

Figure 4. The statistical results of the relation between variations of (a) EB current ($\triangle I_{EB1}$), (b) bias voltages ($\triangle U_{EB}$) and variation of tearing mode frequency ($\triangle f_{TM1}$) in rapid response. Among the results, some data mentioned in figure 3 are contained. The dashed line shows the line of best-fit of rapid response for different positions (by different shapes) and current rise time (by different colors).

To distinguish that the mode frequency varying has a direct correlation with the EB current or bias voltage, the shot-to-shot statistical results of $\triangle f_{TM1}$ versus $\triangle I_{EB1}$ and $\triangle U_{EB1}$ in the rapid response are displayed in figures 4 (a) and (b), respectively. In figure 4(a), there is approximately proportional correlation between variations of TM frequency and EB current, $\triangle f_{TM1}$ =-0.0289$\times\triangle I_{EB1}$-0.0621, which is similar to the relations mentioned above. It is noted that the nonzero value $\triangle f_{TM1}(\triangle I_{EB1}=0)$ = - 0.0621 might be caused by the errors introduced by the acquisition of the data and data fitting. In figure 4(b), the relation between mode frequency and bias voltage is not a proportional correlation, which suggests that the variation of mode frequency has a direct correlation with EB current rather than bias voltage. The result mentioned in paper [1] shows that the mode frequency increases with the more negative bias voltages at the same EB position. In fact, as mentioned in this article, the different bias voltages vary the EB current to change the mode frequency.

The experimental results mentioned above show that the response of mode frequency to EB current contains two processes, rapid response and slow response. In the rapid response, the mode frequency increases with the EB current raising. The mechanism of rapid response is related to the EB current rather than the flow or flow shear around the magnetic island. The qualitative physical mechanism of EB current influencing mode frequency in the rapid response will be discussed in more detail later.

2.3. The dynamics of rapid response of TM to EB current

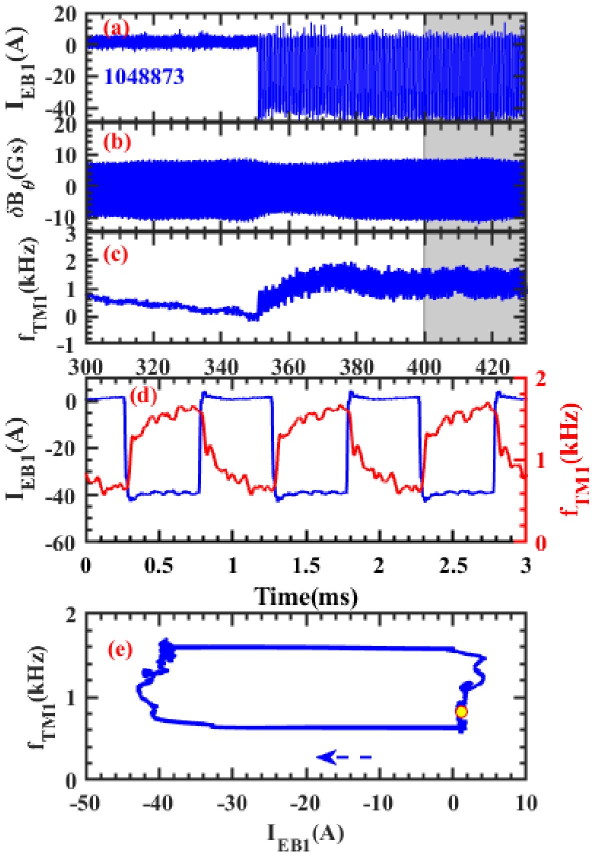

Figure 5. Time evolutions of (a) current of electrode biasing (I_{EB1}, defined in figure 1), (b) poloidal magnetic perturbation (δB_θ), (c) TM frequency (f_{TM1}) for shot 1048873. (d) Auto-conditional average results of EB current (I_{EB1}, shown by blue curve) and TM frequency (f_{TM1}, shown by red curve) for shaded part above. (e) Tearing mode frequency (f_{TM1}) versus EB current (I_{EB1}).

The 1 kHz modulated current is applied to explore the physical mechanism of the rapid response. The experimental waveforms are shown in figures 5(a)-(c). The periodic EB current (as the figure 5(a)) is -43A at 245mm for shot 1048873. There isn't obviously periodic variety for poloidal magnetic perturbation in figure 5(b). The mode frequency modulated by 1 kHz EB current is shown in figure 5(c), which needs detailed analysis. The modulated mode frequency is relatively difficult to distinguish because the modulated current frequency (1 kHz) is close to mode frequency (4 kHz). Another difficulty is that some noise signals are difficult to eliminate because any smooth treatments would make the quickly varying mode frequency, which we concern, distorted. To diminish error and noise of signals, auto-conditional average process is adopted for the shaded part. In this method, every three periods are regarded as a sample, so there are 30 samples in the shaded part. Then the average of 30 samples is calculated to obtain the temporal evolution for mode frequency or EB current (as the figure 5(d)). Detailed analysis shows that the mode frequency increases/decreases periodically as the current turns on/off. The relation between mode frequency and EB current is shown in figure 5(e). The blue arrow means the direction of the loop with the initial point shown by circle. It's found that the mode frequency has a clear delay on EB current. Another result obtained from figure 5(e) is that the response of mode frequency to EB current has good repetition.

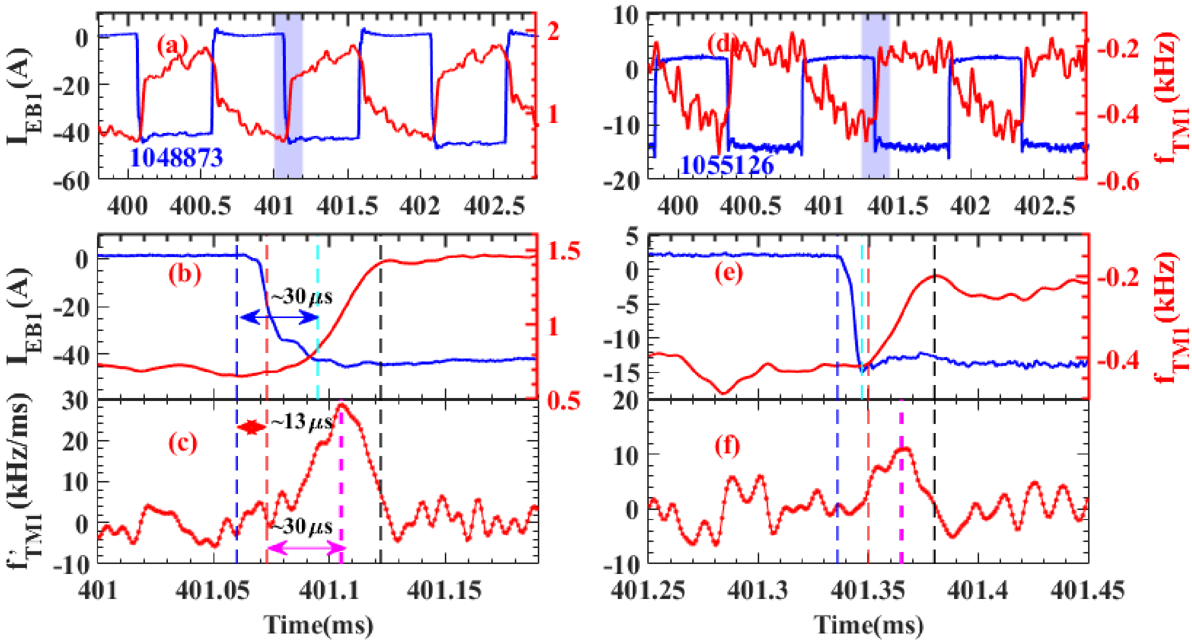

Figure 6. Time evolutions of three cycles' EB current (blue curve) and TM frequency (red curve) (a), (d); (b), (e) detailed analysis of EB current and TM frequency in the shadow part; (c), (f) the derivative of mode frequency in the shaded part for shots 1048873 and 1055126, respectively. The dashed lines mean the moment of: EB current turning on (blue curve), the beginning of mode frequency varying (red curve), EB current ramping to flattop (cyan curve), maximum of frequency derivative (magenta curve), the end of mode frequency varying (black curve), respectively.

The results of 1 kHz modulated mode frequencies with different EB currents for shots 1048873 and 1055126 are shown in figure 6. They are treated in the same way for EB current and mode frequency in figures 6(a) and (d) as method in figure 5 to get the detailed analysis. The shaded parts in figures 6(a) and (d) are analyzed more detailed in figures 6(b), (c) and figures 6(e), (f), respectively. For shot 1048873, the EB current turns on at 400.06ms and ramps to the flattop at about 400.09ms. The mode frequency begins to increase at about 400.073ms, which is about 13μs delay relative to the current varying. The frequency derivative increases gradually, which reveals that the influence on the island is more and more strong, and reaches the maximum at about 400.103ms. The time interval between the beginning of mode frequency increasing and the moment of maximum of frequency derivative is about 30 μs, which is same as the EB current rise time (30 μs). And then, the frequency derivative decreases to near zero at about 400.122ms, which shows that the influence on the island is weaker and weaker and return to approximately initial state occurs at last. There are similar conclusions with lower EB current for shots 1055126. The variation of mode frequency is delayed by about 14 μs with respect to the variation of current. The frequency derivative increases firstly, then declines and goes to near zero at last. The time interval between the beginning of mode frequency increasing and the moment of maximum of frequency derivative is about 15 μs, which is similar to the EB current rise time (13 μs).

In the rapid response, the frequency variation of magnetic island seems to be due to a viscosity effect. The rotation of the magnetic island is accelerated by a viscosity force until the flow shear disappears. However, if the flow shear is initialized by the EB current which is localized between the EB electrode and limiters, it will take a longer time to transport the momentum of flow to the location of magnetic island, which it is longer than the time delay in the above experiments. For this reason, the 'viscosity' could not be caused by the flow shear around the magnetic island. Another interaction mechanism between the EB current and magnetic island will be proposed in the next section and qualitative comparison between the mechanism and experiment will be done.

3. Discussion

In the previous work[31], radial current j_r is induced by the radial electric field E_r between the EB and limiters (or vacuum vessel wall) according to the Ohmic law $\mathrm{E}_r + (\mathrm{v} \times \mathrm{B})_r = \eta_\perp \mathrm{j}_r$ where v is the plasma flow velocity, $\eta_\perp$ is the plasma resistance perpendicular to the magnetic field. The radial current j_r and the magnetic field produce a Lorenz force on the local plasma and drive the plasma poloidal and toroidal rotating acceleration, until a new moment balance between the driving and damping achieved as $\mathrm{j_r} \times \mathrm{B} - \nabla \cdot \Gamma - \mathrm{F}_{\mu\mathrm{v}} = 0$, where Γ is the momentum flux, μ is the damping coefficient. The proportional relationship between the velocity v and the EB current (as the figure 6 in paper [31]) is similar to that between variations of tearing mode frequency ($\triangle f_{TM1}$) and EB current ($\triangle I_{EB1}$) in rapid response in the figure 4. This inspires us that the interaction between the magnetic island and plasma velocity at edge region could be a mechanism of the rapid response.

This interaction is similar to the mode locking process except that the static conductive wall is replaced by the rotating edge plasma layer. At the beginning, when the rotation speed of magnetic island and edge plasma layer are different, the perturbed magnetic field B_r produces an induced current in the rotating plasma layer. Then the induced current and the perturbed magnetic field result in a Lorenz force on the edge plasma layer. Through the conservation of momentum, an opposite Lorenz force would react on the currents, which is the origin of the perturbed magnetic field. This couple of Lorenz force tends to keep the rotation angular speed of magnetic island and edge plasma layer the same. Whether the magnetic island rotation is accelerated or decelerated depends on the rotation difference between the rotation of magnetic island and edge plasma layer.

In this work, the magnetic island rotates at the direction of electron diamagnetic drift. When EB current j_r is directed to the plasma core ($\triangle I_{EB1}<0$), the edge plasma layer is accelerated in the direction of electron diamagnetic drift and could drag the magnetic island to rotate faster through the couple of Lorenz force, which results in the increase of tearing mode frequency as shown in the figure 4, and vice versa. As the current value is higher, the edge plasma layer rotates faster and enhances the induced current and so as to the Lorenz force, which could accelerate the magnetic island more sensitively. It is consistent to the results in the figure 6. From another aspect, this acceleration process starts as soon as the turn-on of EB system and effect the magnetic island frequency much more quickly than the momentum transport process. From the above, the direct interaction between the magnetic island and edge plasma layer could be a candidate mechanism for the rapid response of 2/1 tearing mode to electrode biasing.

A different explanation mentioned in paper [36] is that the stabilization of tearing mode is attributed to global current profile changing induced by local application of electric potential. The global current profile changing is relevant to the improvement of plasma confinement, so the time scale of global current profile changing is similar to that of the momentum transport. However, in rapid process, the EB current affects the magnetic island frequency much more quickly than the momentum transport process. Therefore, in the experiments considered here, the mechanism is not so important in rapid response.

Another explanation is that the effect on the tearing mode is attributed to a coupling between the m/n = 2/1 magnetic islands and the halo-current magnetic field, in which the mechanism is ascribed to resonant magnetic perturbation (RMP)[37, 38]. The halo-current loop consists of a rail limiter, plasma SOL, vacuum vessel, and external part of the circuit[37, 38]. In the experiments considered here, when the EB is at the plasma boundary surface (P_{EB} = 255mm in figure 3(c)), the EB current mostly goes around the magnetic field line at the plasma boundary surface and flows back through the limiters. The radial current component is small. So the current circuit is similar to halo-current loop. While the EB is into the plasma (P_{EB} = 240\245\250mm in figure 3(c)), the EB current must go across the flux surface to arrive at the plasma boundary surface and flow back through the limiters. The current circuit can be expected to consist of radial current and halo-current loop. As shown in figure 3(c), the variation of mode frequency when the EB is at the plasma boundary surface is much smaller than that when the

EB is placed into the plasma. Therefore, the radial current plays a more important role than halo current in the rapid response here. Although the electrode biasing probe could introduce a magnetic field perturbation and can be expected to act as a resonant magnetic perturbation, the dependence of the results on halo current and the bias polarity suggest that the RMP nature of the probe is subdominant and negligible in the experiments considered here.

4. Summary

The effect of electrode biasing on the m/n = 2/1 tearing mode has been experimentally studied in J-TEXT tokamak. According to the response time, the response of 2/1 tearing mode frequency to EB can be divided into two processes: the rapid response and the slow response. A question mentioned in paper [1], which is that the TM frequency decouples from the toroidal rotation speed V_Φ when turning on/off the EB voltage, is settled. In the rapid response, experimental results show that the variation of mode frequency is ahead of that of plasma rotation around the magnetic island, which reveals that the variation of mode frequency has little relation on plasma flow or flow shear around the magnetic island. In the experiments considered, the proportionality coefficient between TM frequency and EB current is a constant no matter how much are the electrode position, bias voltage, and the EB current rise time varied in the rapid response. The rapid response proportionality of TM frequency to EB current is similar to the proportional relationship between the velocity v and the EB current in [31] (the figure 6 in [31]). The detailed analysis of physical mechanism of EB current influencing mode frequency in the rapid response is obtained by auto-conditional average. The modulated mode frequency is synchronous with the EB current. There is an about 13 μs delay between variations time of mode frequency and EB current, which is much more quickly than time of momentum transport process.

The heuristic mechanism for the rapid response of 2/1 tearing mode to electrode biasing is similar to mode locking process except that the static conductive wall is replaced by the edge rotating plasma layer. The rotation difference between magnetic island and edge plasma layer will induce a couple of Lorenz force to keep the rotation of magnetic island and edge plasma layer the same. So whether the magnetic island rotation is accelerated or decelerated depends on the rotation difference between the rotation of magnetic island and edge plasma layer. The negative EB current would increase the rotation of edge plasma layer and then the magnetic island is dragged by Lorenz force.

The results mentioned above reveal that the mode frequency can be modulated by EB current in a small amount of time. The high enough negative bias voltage, which generates enough current, can increase the 2/1 TM frequency in time during the rapid response. And then the 2/1 TM frequency could be suppressed completely (as the figure 4 in paper [1]) during the slow response. Application of electrode biasing possibly is an effective method to avoid mode locking or unlock the locked mode.

Acknowledgments

The authors would like to thank the members of the J-TEXT team for their assistance in the experiment. This work is supported by National Magnetic Confinement Fusion Science Program of China under contract No. 2015GB111001 and the National Natural Science Foundation of China (Contract No. 11305070 and 11505069).

References

[1] LIU H, HU Q, CHEN Z, et al. Effect of electrode biasing onm/n = 2/1 tearing modes in J-TEXT experiments [J]. Nuclear Fusion, 2017, 57(1): 016003.
[2] CHU M S, CHEN L, ZHENG L-J, et al. Effect of rotation on ideal and resistive MHD modes [J]. Nuclear Fusion, 1999, 39(p): 2107.
[3] WEI L, WANG Z-X. Roles of poloidal rotation in the q = 1 high-order harmonic tearing modes in a tokamak plasma [J]. Physics of Plasmas, 2013, 20(1): 012512.
[4] CHAPMAN I T, BROWN S, KEMP R, et al. Toroidal velocity shear Kelvin–Helmholtz

instabilities in strongly rotating tokamak plasmas [J]. Nuclear Fusion, 2012, 52(4): 042005.
[5] BIERWAGE A, YU Q, GüNTER S. Large-mode-number magnetohydrodynamic instability driven by sheared flows in a tokamak plasma with reversed central shear [J]. Physics of Plasmas, 2007, 14(1): 010704.
[6] OFMAN L, CHEN X L, MORRISON P J, et al. Resistive tearing mode instability with shear flow and viscosity [J]. Physics of Fluids B: Plasma Physics, 1991, 3(6): 1364-73.
[7] CHEN X L, MORRISON P J. Resistive tearing instability with equilibrium shear flow [J]. Physics of Fluids B: Plasma Physics, 1990, 2(3): 495-507.
[8] WANG X, BHATTACHARJEE A, MA Z W, et al. Structure and dynamics of current sheets at Alfvén resonances in a differentially rotating plasma [J]. Physics of Plasmas, 1998, 5(6): 2291-6.
[9] REN C, CHU M S, CALLEN J D. Magnetic island deformation due to sheared flow and viscosity [J]. Physics of Plasmas, 1999, 6(4): 1203-7.
[10] HU Q, YU Q, HU X. Linear and nonlinear effect of sheared plasma flow on resistive tearing modes [J]. Physics of Plasmas, 2014, 21(12): 122507.
[11] CHANDRA D, SEN A, KAW P, et al. Effect of sheared flows on classical and neoclassical tearing modes [J]. Nuclear Fusion, 2005, 45(6): 524-30.
[12] COELHO R, LAZZARO E. Effect of sheared equilibrium plasma rotation on the classical tearing mode in a cylindrical geometry [J]. Physics of Plasmas, 2007, 14(1): 012101.
[13] KEILHACKER M, TEAM J. Fusion physics progress on the Joint European Torus (JET) [J]. Plasma Physics & Controlled Fusion, 1999, 41(12): B1-B23().
[14] LUXON J L. A design retrospective of the DIII-D tokamak [J]. Nuclear Fusion, 2002, 42(5): 614-33.
[15] ONO M, KAYE S M, PENG Y K M, et al. Exploration of spherical torus physics in the NSTX device [J]. Nuclear Fusion, 2000, 40(3): 557-61.
[16] LA HAYE R J, BUTTERY R J. The stabilizing effect of flow shear on m/n=3/2 magnetic island width in DIII-D [J]. Physics of Plasmas, 2009, 16(2): 022107.
[17] LA HAYE R J, BRENNAN D P, BUTTERY R J, et al. Islands in the stream: The effect of plasma flow on tearing stability [J]. Physics of Plasmas, 2010, 17(5): 056110.
[18] LA HAYE R J, PETTY C C, POLITZER P A. Influence of plasma flow shear on tearing in DIII-D hybrids [J]. Nuclear Fusion, 2011, 51(5): 053013.
[19] BUTTERY R J, LA HAYE R J, GOHIL P, et al. The influence of rotation on the βN threshold for the 2 / 1 neoclassical tearing mode in DIII-D [J]. Physics of Plasmas, 2008, 15(5): 056115.
[20] GERHARDT S P, BRENNAN D P, BUTTERY R, et al. Relationship between onset thresholds, trigger types and rotation shear for them/n= 2/1 neoclassical tearing mode in a high-β spherical torus [J]. Nuclear Fusion, 2009, 49(3): 032003.
[21] TAYLOR R J, BROWN M L, FRIED B D, et al. H-mode behavior induced by cross-field currents in a tokamak [J]. Phys Rev Lett, 1989, 63(21): 2365-8.
[22] TAYLOR R J. Macrotor physics and technology results [J]. Nuclear Fusion, 1985, 25(25): 1173.
[23] ASKINAZI L G, GOLANT V E, LEBEDEV S V, et al. Radial current in a tokamak caused by a biased electrode [J]. 1992, 32(2): 271.
[24] DHYANI P, GHOSH J, CHATTOPADHYAY P K, et al. A novel approach for mitigating disruptions using biased electrode in Aditya tokamak [J]. Nuclear Fusion, 2014, 54(8): 083023.
[25] GHORANNEVISS M, SALAR ELAHI A, TAJDIDZADEH M, et al. Design, Construction, and Installation of Movable Electrode Biasing System on Tokamak [J]. Journal of Fusion Energy, 2010, 29(5): 467-70.

[26]NASCIMENTO I C, KUZNETSOV Y K, GUIMARãES-FILHO Z O, et al. Suppression and excitation of MHD activity with an electrically polarized electrode at the TCABR tokamak plasma edge [J]. Nuclear Fusion, 2007, 47(11): 1570-6.
[27]LU H W, LUO J R, ZHONG F C, et al. Suppression of MHD activity with limiter biasing in the HT-7 tokamak [J]. The European Physical Journal D, 2012, 66(8):
[28]GHASEMLOO M, GHORANNEVISS M, SALEM M K. The effect of biased limiter on the magnetic island width in tokamak plasma [J]. Journal of Plasma Physics, 2013, 80(01): 113-30.
[29]ZHU T Z, CHEN Z P, SUN Y, et al. The construction of an electrode biasing system for driving plasma rotation in J-TEXT tokamak [J]. The Review of scientific instruments, 2014, 85(5): 053504.
[30]SUN Y, CHEN Z P, ZHU T Z, et al. The influence of electrode biasing on plasma confinement in the J-TEXT tokamak [J]. Plasma Physics and Controlled Fusion, 2014, 56(1): 015001.
[31]SUN Y, CHEN Z P, ZHUANG G, et al. Investigations of turbulent transport and intrinsic torque of toroidal momentum at the edge of J-TEXT tokamak with electrode biasing [J]. Nuclear Fusion, 2016, 56(4): 046006.
[32]ZHUANG G, GENTLE K W, CHEN Z Y, et al. Progress of recent experimental research on the J-TEXT tokamak [J]. Nuclear Fusion, 2017, 57(10): 102003.
[33]CHENG Z F, LUO J, WANG Z J, et al. Edge impurity rotation profile measurement by using high-resolution ultraviolet/visible spectrometer on J-TEXT [J]. The Review of scientific instruments, 2014, 85(11): 11E423.
[34]RAJU D, JHA R, KAW P K, et al. Mirnov coil data analysis for tokamak ADITYA [J]. Pramana Journal of Physics, 2000, 55(5-6): 727-32.
[35]YANG Z J, PHILLIPS P E, ZHUANG G, et al. A 16-channel heterodyne electron cyclotron emission radiometer on J-TEXT [J]. The Review of scientific instruments, 2012, 83(10): 10E313.
[36]BASU D, PAL R, MARTINELL J J, et al. Disruption avoidance in the SINP-Tokamak by means of electrode-biasing at the plasma edge [J]. Physics of Plasmas, 2013, 20(5):
[37]CHUDNOVSKIY A N J N F. MHD-Mode Locking by Controlled Halo-Current in T-10 Tokamak [J]. 2003, 43(8): 681---685685.
[38]IVANOV N V, KAKURIN A M. Simulation of magnetic island dynamics under resonant magnetic perturbation with the TEAR code and validation of the results on T-10 tokamak data [J]. Physics of Plasmas, 2014, 21(10):